International Journal of Engineering & Technology, 7 (3.11) (2018) 34-37

International Journal of Engineering & Technology

Website: www.sciencepubco.com/index.php/IJET

Research paper

The Effects of Sn-Doping on a-Fe_2O_3 Nanostructures Properties

W.R.W. Ahmad[1]*, M.H. Mamat[1,2], A.S. Zoolfakar[1], Z. Khusaimi[2], M.M. Yusof[1], A.S. Ismail[1], S.A. Saidi[1], M. Rusop[1,2]

[1]NANO-ElecTronic Centre (NET), Faculty of Electrical Engineering, Universiti Teknologi MARA (UiTM), 40450 Shah Alam, Selangor, Malaysia

[2]NANO-SciTech Centre, Institute of Science, Universiti Teknologi MARA, 40450 Shah Alam, Selangor, Malaysia

**Corresponding author E-mail: rosmaria@salam.uitm.edu.my*

Abstract

In this study, undoped and Sn-doped hematite (α-Fe_2O_3) nanostructures with variation of Sn (0.5, 1, 2, 3 at. %) were deposited on fluorine doped tin oxide (FTO) coated glass substrate using sonicated immersion method. The effect of Sn-dopant on structural and crystallinity properties were investigated by characterizing FESEM and XRD respectively, while the optical properties were measured by UV-Vis-NIR spectrometer. The surface morphologies from FESEM have shown that the hematite nanostructures were grown uniformly in all samples. However, as the dopant atomic percentage increases, the amount of hematite nanostructure being grown on the FTO decreases. Results demonstrated that the amount of Sn-doping was undoubtedly influence the structural, optical and electrical properties of hematite nanostructures.

Keywords: *Hematite, hematite nanostructure, Sn-doped α-Fe_2O_3, sonicated immersion*

1. Introduction

Hematite (α-Fe_2O_3) is one of the minerals resulting from the composition of several iron oxides. It becomes essential in semiconductor industry nowadays due to its advantages such as nontoxic, abundant, and low cost. Apart of being as an n-type semiconductor with the bandgap of 2.1 eV, hematite is thermodynamically stable structure under ambient conditions. This metal oxide has been used in wide applications such as photoelectrochemical water splitting[1]–[4], gas sensors[5], [6], lithium-ion batteries[7], and magnetism[8]. In developing the material elements in electronic devices, hematite can be prepared by different deposition techniques for example spin coating deposition[9], DC magnetron sputtering[10], and solution based methods such as sol gel, electrochemical depositions[3] and hydrothermal[11], [12]. Among these techniques, solution-based methods have evolved as a promising method because of their low cost, simplicity, and its ability to produce excellent nanorod structures. Variety of synthesis methods also contribute to produce different type of hematite nanostructures includes nanotubes[13], nanowires[14], hollow structures[10], nanorods[7], [15], and flower-like nanostructures[4]. Nanorods structure reveals a unique properties and strong potential for sensor applications. These are due to the larger surface area which contributes to higher carrier transferability in sensor devices [16], [17]. Recently, numerous researches on developing hematite nanorod arrays are concentrating on using hydrothermal technique, which is accompanying with a few drawbacks include higher temperature, higher pressure, and longer synthesis process. These are consequently causing higher cost involved that we are trying to avoid.

The pristine α-Fe_2O_3 has many limitations in many applications due to its poor electrical properties. Neri et. al. [18] have investigated the effects of Li^+, Zn^{2+}, and Au^{3+} as humidity sensing materials and found that the sensor characteristics of the doped sensing materials are correlated to the charge density and the concentration of the dopants on the surface. In other study that using tin (Sn) doping, Orlandi et. al. [6] has investigated the effects of Sn doped hematite that were fabricated using radio-frequency magnetron sputtering with subsequent high temperature (800°C) treatment, and found that the presence of Sn in hematite enhances the compatibility of the device towards substrate. Moreover, the Sn ions induce lattice distortion with the increase of cell volume. A few studies have reported on the effects of other dopants on the hematite (α-Fe_2O_3) structural and electrical properties for through different approach[1], [19]–[21].

Sn^{4+} ion has a comparable ionic radius as an effective dopant for α-Fe_2O_3. By adding M^{4+} ions to α-Fe_2O_3, it modifies the structural, optical and electrical properties of hematite. Sn^{4+} ion substitutes Fe^{3+} in hematite which enhances the electron transferability by increasing its electrical conductivity. The hematite is well-known has significant applications in photocatalysis, gas sensors, lithium ion battery, photoelectrochemical water splitting, humidity sensor, etc. Most of the works investigated the pristine and doped hematite nanostructures using hydrothermal synthesis. To the best of our knowledge, there are no reports on the study of tin-doped hematite nanostructure that synthesized using solution base method.

In this work, we investigate the effect of Sn-doped hematite through a solution-based method i.e. sonicated immersion method. The synthesis method was chosen due to its low-cost synthesis route, simplicity of the process, and the feasibility of producing sensing film on the substrates compared to hydrothermal synthesis that requires high temperature, high pressure and longer synthesis duration.

Copyright © 2018 Authors. This is an open access article distributed under the Creative Commons Attribution License, which permits unrestricted use, distribution, and reproduction in any medium, provided the original work is properly cited.

2. Experimental Work

In substrate preparation, fluorine tin oxide (FTO) coated glass substrates was used as substrate to form hematite nanostructure film. These conductive and transparent glass substrates need to be cleaned prior to be used in synthesis process to remove the contaminations on the substrate surface. The substrates with 2cm x 2cm in size were placed in a beaker that contain methanol (CH_3OH) and covered with aluminium foil. Then the beaker was sonicated in an ultrasonic cleanser for 10 minutes at 50°C. The FTO substrates then were cleaned with DI water and were sonicated again in DI water for 10 minutes at 50°C. After cleaning process, the FTO substrates were dried prior to the synthesis process.

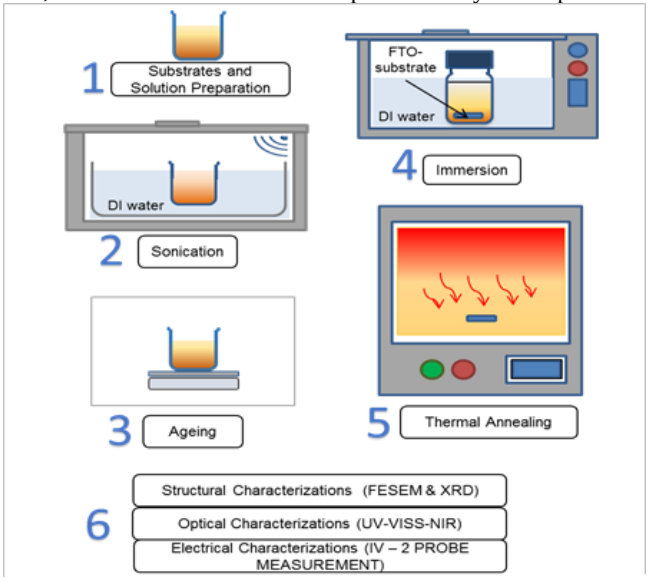


Fig. 1: The synthesis process involved in sonicated immersion method (1-5) and followed with the characterizations (6).

Sonicated immersion method was used as the method for synthesizing the undoped and Sn-doped hematite. The synthesis method involves a few substances, 0.2 M ferric chloride ($FeCl_3{\cdot}6H_2O$) as precursor, 0.2M of urea (NH_2CONH_2) as stabilizer, DI water as solvent and tin (Sn) as the dopant. All these reagents were mixed together in five different beakers with the atomic percentage (at. %) of Sn dopant varied at 0 (undoped sample), 0.5, 1.0, 2.0, and 3.0 at. %. All the samples in each beaker were sonicated in ultrasonic waterbath for 30 minutes at 50°C, and then the solutions were stirred (ageing) for 5 minutes at 250rpm under room temperature on a hot plate. The FTO glass substrates were placed in all Schott bottles whereas the conductive side of the substrates facing upwards. The non-conductive sides of the FTO were taped to prevent the growth of hematite nanostructures on the region for contact purpose. Next, the solution mixture was poured into the Schott bottles and immersed in water bath equipment for two hours at 95°C. After immersion process, the samples were dried for 10 minutes at 150°C in a furnace followed by annealed at 500°C for 1 hour afterwards. At this condition, the samples are ready for structural and optical characterizations. The synthesis characterizations processes involved in this work are illustrated as in Fig. 1. The obtained hematite nanostructure is expected as figured in Fig. 2, whereby the hematite is grown on the FTO conductive layer on the glass substrate. For electrical characterization, the samples were deposited with silver (Ag) contact through thermal evaporation process.

The general morphology of hematite samples was examined by Field Emission Scanning Electron Microscopy (FESEM; JEOL JSM-7600F) and the crystallinity was measured through X-Ray Diffraction (XRD; PANalytical X'Pert PRO). The optical properties were characterized by Ultraviolet Visible Spectroscopy (Varian Cary 5000). The electrical properties were characterized by using 2-probe IV Measurement system with an applied voltage range in 10V.

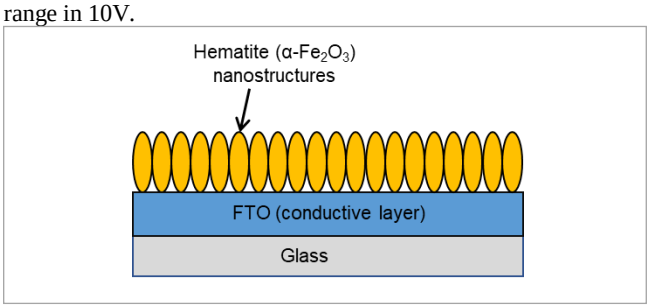


Fig. 2: The structure of hematite nanostructure grown on FTO coated glass substrate

3. Results and Discussions

The crystallinity properties of the hematite nanostructures were characterized using X-ray diffraction (XRD) to observe the crystalline structure of as-prepared hematite samples. In this analysis, XRD patterns for undoped and doped samples were indicated as in Fig. 3. It is observed that the XRD patterns of the films are resemble to main diffraction peaks of hematite phase, precisely, (012), (110), (116), (214), and (125), which attributed to a polycrystalline structure with rhombohedral lattice system. These patterns are in consistent with the reported value (JCPDS #00-033-0664). In the XRD pattern, no other phases of metal oxides such as meghemite (γ-Fe_2O_3) and magnetite (Fe_3O_4) were observed. The highest peak (with high intensity) at 38° of 2θ was observed in the XRD pattern down to X-ray penetration into the FTO conductive layer on the glass substrate.

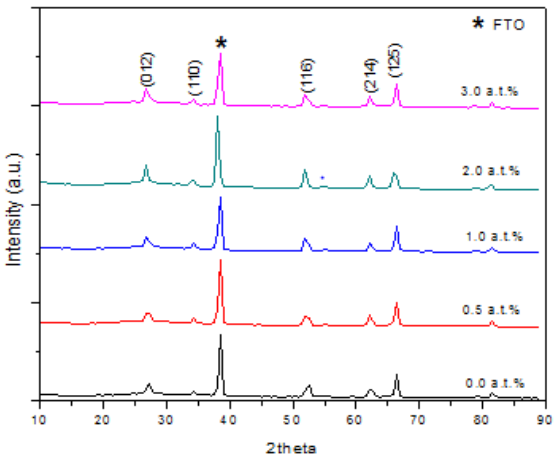


Fig. 3: XRD patterns of undoped and Sn-doped α-Fe_2O_3 nanostructures for different dopant after thermal annealing treatment at 500°C for 1 hour.

The surface morphology of the undoped and Sn-doped hematite samples were observed by using Field Emission Scanning Electron Microscopy (FESEM). Fig. 4 presents the FESEM images of undoped and another two samples of Sn-doped α-Fe_2O_3 with different at. % of Sn dopant. Fig. 4 (a),(c),and (e) shows the FESEM images of undoped (0.0 at. %), 1.0 at. % Sn-doped and 3.0 at. % Sn-doped α-Fe_2O_3 at 50,000x magnification, as which indicating a uniform deposition of hematite nanostructure deformed on the FTO glass substrate. However, the high magnification (150,000x) FESEM shown in Fig. 4(b), (d), and (f) reveals that the growth of hematite nanostructures was decreased as the amount of Sn is increased. There are merely few nanorods were adhered to the FTO conductive layer which is possibly cause very high current flow through the device. For the undoped sample, the structure grows clearly but for the Sn-doped 3 at. %, the nanostructure was not clearly formed. Thus, when the Sn dopant at. % is increased, the nanostructure film is decrease in number and the uniformity also decreased.

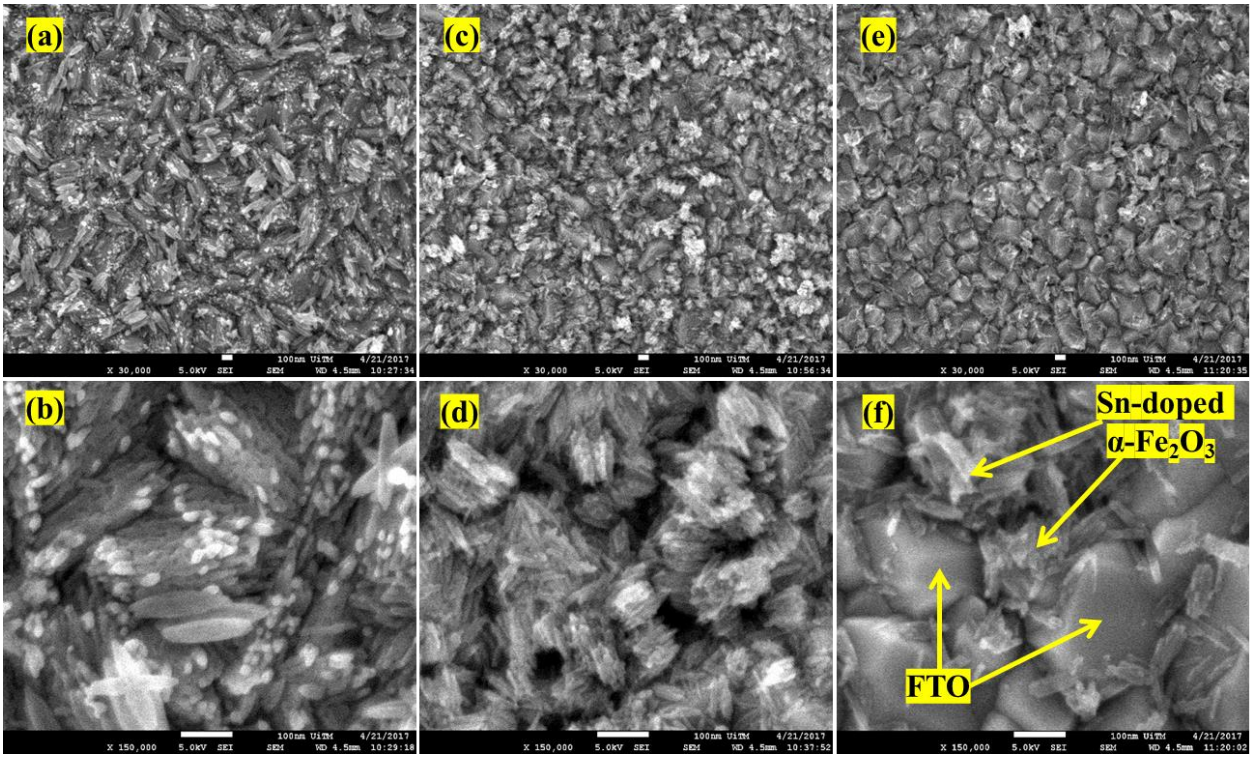


Fig. 4: FESEM images of (a) undoped α-Fe_2O_3, (c) 1 at. % Sn-doped α-Fe_2O_3, (e) 3 at. % Sn-doped α-Fe_2O_3 at 30,000x magnification, meanwhile (b) undoped α-Fe_2O_3, (d) 1 at. % Sn-doped α-Fe_2O_3, and (f) 3 at. % Sn-doped α-Fe_2O_3 at 150,000x magnification.

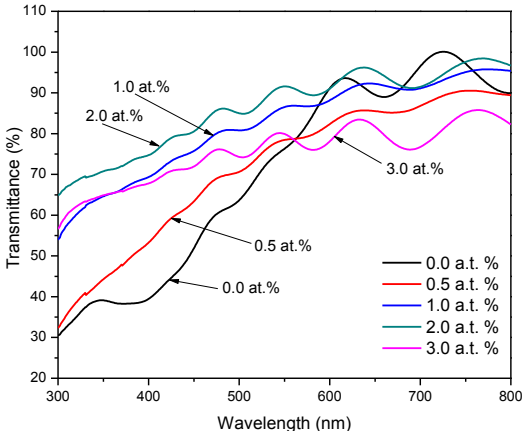


Fig. 5: Transmittance properties of undoped (0.0 at. %), and Sn-doped α-Fe_2O_3 for different at. %

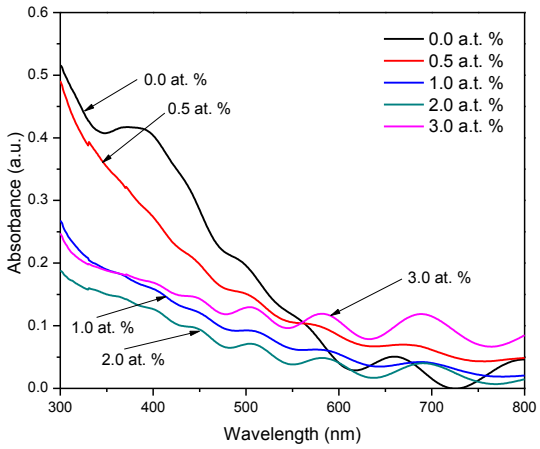


Fig. 6: Absorbance properties of undoped (0.0 at. %), and Sn-doped α-Fe_2O_3 for different at. %

The optical properties were determined using Ultraviolet Visible (UV-Vis) Spectroscopy to investigate the behaviour of transmittance and absorbance properties in the visible range (300-800nm wavelength). The transmittance and absorbance profiles of undoped and Sn-doped hematite nanostructures are indicated in Fig. 5, and Fig. 6 respectively. In the case of high Sn doping (0.5, 1, 2, 3 at. %), the optical UV-VIS-NIR display a reduced absorption in the entire investigated ranges rather than the undoped hematite sample does. However, the hematite sample with 0.5 at. % has shown approaching values of optical properties to the undoped hematite sample. Moreover, the optical properties demonstrate the undoped sample has the highest transmittance at 700nm wavelength. The difference in optical properties is probably due to less deposition of the hematite nanostructure onto FTO substrate due to the presence of higher volume of Sn in the solution mixture. These might cause by the scattering effect in the hematite samples.

The electrical properties of the undoped and Sn-doped hematite were measured by using 2-probe IV measurement equipment. The output profile of IV for all samples is indicated in Fig. 7. It is clearly can be observed that the samples of undoped and Sn-doped 0.5 at. % display a typical Ohmic behavior whereby the current values linearly increased with the increment of the voltages. On the other hand, the undoped hematite exhibits low n-type conductivity due to low carrier concentration in the thin film. The fast increment of current in sample with Sn-doped 0.5 at. % and 3 at. % are undoubtedly due to very thin layer of hematite nanostructures grown on FTO substrate that causing a very high current flow.

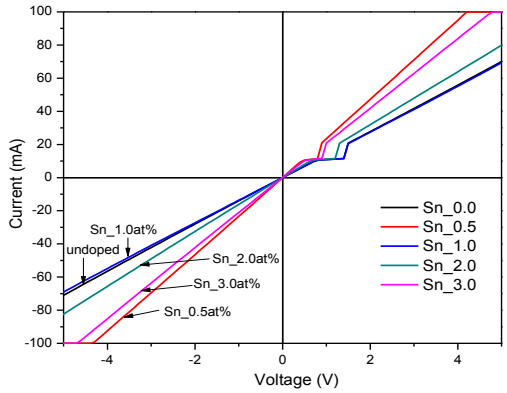


Fig. 7: I-V characteristics of undoped and Sn-doped hematite with different at. %.

4. Conclusion

Tin (Sn) doped hematite (α-Fe_2O_3) nanostructures were successfully prepared on the FTO coated glass substrate by using sonicated immersion method. The structural, optical and electrical properties of Sn-doped hematite have been investigated by varying the amount of Sn dopant ranging 0-3 at. %. The prepared Sn-doped α-Fe_2O_3 reveals that the properties of hematite can be controlled by adding dopant with appropriate amount. The Sn dopant approximately 0.5 at. % is needed to improve the structural, optical and electrical properties of hematite. The volume of hematite nanostructure grown on the FTO substrate reduced when the atomic percentage of dopant is increased. This suggest that further optimization with smaller range of at. % is constructive to improve the electronic properties of hematite, thus the sensor measurement to examine the potential of Sn-doped α-Fe_2O_3 to be applied as a sensor element in electronic devices. Further investigation also can be carried out on varying the annealing temperature up to 800°C to investigate if the hematite nanostructures need higher temperature treatment to overcome the defects in the hematite crystal structure.

Acknowledgement

This work was supported by the LESTARI grant (600-IRMI/MYRA5/3/LESTARI (0162/2016)) from Universiti Teknologi MARA (UiTM), Malaysia. The authors also would like to thank the Research Management Institute (RMI) of UiTM for financial management support of this research.

References

[1] A. Subramanian *et al.*, "Effect of tetravalent dopants on hematite nanostructure for enhanced photoelectrochemical water splitting," *Appl. Surf. Sci.*, vol. 427, pp. 1203–1212, 2018.

[2] A. Annamalai *et al.*, "Fabrication of superior α-Fe2O3 nanorod photoanodes through ex-situ Sn-doping for solar water splitting," *Sol. Energy Mater. Sol. Cells*, vol. 144, pp. 247–255, 2016.

[3] Q. Meng, Z. Wang, X. Chai, Z. Weng, R. Ding, and L. Dong, "Fabrication of hematite (α-Fe2O3) nanoparticles using electrochemical deposition," *Appl. Surf. Sci.*, vol. 368, pp. 303–308, 2016.

[4] E. L. Tsege, T. S. Atabaev, M. A. Hossain, D. Lee, H. K. Kim, and Y. H. Hwang, "Cu-doped flower-like hematite nanostructures for efficient water splitting applications," *J. Phys. Chem. Solids*, vol. 98, pp. 283–289, 2016.

[5] B. Lucas-granados, R. Sánchez-tovar, R. M. Fernández-domene, and J. García-antón, "Applied Surface Science Controlled hydrodynamic conditions on the formation of iron oxide nanostructures synthesized by electrochemical anodization : Effect of the electrode rotation speed," *Appl. Surf. Sci.*, vol. 392, pp. 503–513, 2017.

[6] M. Orlandi *et al.*, "On the effect of Sn-doping in hematite anodes for oxygen evolution," *Electrochim. Acta*, vol. 214, pp. 345–353, 2016.

[7] M. Balogun *et al.*, "High power density nitridated hematite (α-Fe2O3) nanorods as anode for high-performance flexible lithium ion batteries," *J. Power Sources*, vol. 308, pp. 7–17, Mar. 2016.

[8] N. Pariona, K. I. Camacho-Aguilar, R. Ramos-González, A. I. Martinez, M. Herrera-Trejo, and E. Baggio-Saitovitch, "Magnetic and structural properties of ferrihydrite/hematite nanocomposites," *J. Magn. Magn. Mater.*, vol. 406, pp. 221–227, 2016.

[9] F. L. Souza, K. P. Lopes, P. A. P. Nascente, and E. R. Leite, "Nanostructured hematite thin films produced by spin-coating deposition solution: Application in water splitting," *Sol. Energy Mater. Sol. Cells*, vol. 93, no. 3, pp. 362–368, 2009.

[10] M. C. Huang, T. Wang, C. C. Wu, W. S. Chang, J. C. Lin, and T. H. Yen, "The optical, structural and photoelectrochemical characteristics of porous hematite hollow spheres prepared by DC magnetron sputtering process via polystyrene spheres template," *Ceram. Int.*, vol. 40, no. 7 PART B, pp. 10537–10544, 2014.

[11] R. Rajendran, Z. Yaakob, M. Pudukudy, M. S. A. Rahaman, and K. Sopian, "Photoelectrochemical water splitting performance of vertically aligned hematite nanoflakes deposited on FTO by a hydrothermal method," *J. Alloys Compd.*, vol. 608, pp. 207–212, 2014.

[12] A. Pu, J. Deng, Y. Hao, X. Sun, and J. Zhong, "Thickness effect of hematite nanostructures prepared by hydrothermal method for solar water splitting," *Appl. Surf. Sci.*, vol. 320, pp. 213–217, 2014.

[13] L. Chen, H. Xu, L. Li, F. Wu, J. Yang, and Y. Qian, "A comparative study of lithium-storage performances of hematite: Nanotubes vs. nanorods," *J. Power Sources*, vol. 245, pp. 429–435, 2014.

[14] S. Grigorescu *et al.*, "Thermal air oxidation of Fe: Rapid hematite nanowire growth and photoelectrochemical water splitting performance," *Electrochem. commun.*, vol. 23, no. 1, pp. 59–62, 2012.

[15] P. S. Bassi, R. P. Antony, P. P. Boix, Y. Fang, J. Barber, and L. H. Wong, "Crystalline Fe2O3/Fe2TiO5 heterojunction nanorods with efficient charge separation and hole injection as photoanode for solar water oxidation," *Nano Energy*, vol. 22, pp. 310–318, 2016.

[16] M. H. Mamat *et al.*, "Fabrication of Intrinsic Zinc Oxide-Coated , Aluminium-Doped Zinc Oxide Nanorod Array-Based Ultraviolet Photoconductive Sensors," no. February 2016, pp. 6–8, 2015.

[17] A. S. Ismail *et al.*, "Fabrication of hierarchical Sn-doped ZnO nanorod arrays through sonicated sol–gel immersion for room temperature, resistive-type humidity sensor applications," *Ceram. Int.*, 2016.

[18] G. Neri, a. Bonavita, S. Galvagno, N. Donato, and a. Caddemi, "Electrical characterization of Fe2O3 humidity sensors doped with Li+, Zn2+ and Au3+ ions," *Sensors Actuators B Chem.*, vol. 111–112, pp. 71–77, 2005.

[19] K. D. Malviya, H. Dotan, D. Shlenkevich, A. Tsyganok, H. Mor, and A. Rothschild, "Systematic comparison of different dopants in thin film hematite (α-Fe2O3) photoanodes for solar water splitting," *J. Mater. Chem. A Mater. energy Sustain.*, vol. 4, pp. 3091–3099, 2016.

[20] A. S. Afify *et al.*, "Studying the effect of doping metal ions onto a crystalline hematite-based humidity sensor for environmental control," *Bulg. Chem. Commun.*, vol. 48, no. 2, pp. 297–302, 2016.

[21] H. J. Song, Y. Sun, and X. H. Jia, "Hydrothermal synthesis, growth mechanism and gas sensing properties of Zn-doped α-Fe2O3 microcubes," *Ceram. Int.*, vol. 41, no. 10, pp. 13224–13231, 2015.

[22] K. Bindu, K. M. Ajith, and H. S. Nagaraja, "Electrical, dielectric and magnetic properties of Sn-doped hematite (a-SnxFe2-xO3) nanoplates synthesized by microwave-assisted method," *J. Alloys Compd.*, vol. 735, pp. 847–854, 2018.